THE ASTROPHYSICAL JOURNAL, 469:944–953, 1996 October 1

DISRUPTION OF HELMET STREAMERS BY CURRENT EMERGENCE

W. P. GUO AND S. T. WU
Center for Space Plasma and Aeronomic Research, Department of Mechanical and Aerospace Engineering, University of Alabama in Huntsville, Huntsville, AL 35899

AND

E. TANDBERG-HANSSEN
Space Sciences Laboratory, NASA/Marshall Space Flight Center, Huntsville, AL 35812
Received 1995 September 25; accepted 1996 April 16

ABSTRACT

We have investigated the dynamic response of a coronal helmet streamer to the emergence from below of a current with its magnetic field in a direction opposite to the overlying streamer field. Once the emerging current moves into the closed region of the streamer, a current sheet forms between the emerging field and the streamer field, because the preexisting field and the newly emerging field have opposite polarities. Thus magnetic reconnection will occur at the flanks of the emerged structure where the current density is maximum. If the emerging current is large enough, the energy contained in the current and the reconnection will promptly disrupt the streamer. If the emerging current is small, the streamer will experience a stage of slow evolution. In this stage, slow magnetic reconnection occurring at the flanks of the emerged structure leads to the degeneration of the emerged current to a neutral point. Above this point, a new magnetic bubble will form. The resulting configuration resembles an inverse-polarity prominence. Depending on the initial input energy of the current, the resulting structure will either remain in situ, forming a quasi-static structure, or move upward, forming a coronal transient similar to coronal jets. The numerical method used in this paper can be used to construct helmet streamers containing a detached magnetic structure in their closed field region. The quasi-static solution may serve as a preevent corona for studying coronal mass ejection initiation.

Subject headings: MHD — Sun: corona — Sun: prominences

1. INTRODUCTION

Considerable interest and work have recently been devoted to studying the complex interaction of coronal helmet streamers, coronal mass ejections (CMEs), and erupting prominences. The equilibrium of large-scale, quasi-static helmet streamers seems to be closely associated with the occurrence of many CMEs (e.g., Illing & Hundhausen 1986; Hundhausen 1993), and the "disparition brusque" phase of prominences normally takes place in changing helmet streamers (e.g., Tandberg-Hanssen 1995). Different aspects of these interactions have been treated in the literature, but the complexity of the problem generally requires serious simplifications in the applied physical models.

It is difficult to construct helmet-streamer solutions analytically from MHD equations because both static, magnetically dominated closed regions and flow-dominated, open regions occur. Pneuman & Kopp (1971) first obtained a numerical solution for a helmet streamer using an iterative procedure. Since then, a more general relaxation method has been used to obtain quasi-static helmet streamers (Steinolfson, Suess, & Wu 1982; Wang et al. 1993). It has been demonstrated that the helmet streamer is a better initial state for simulating looplike coronal mass ejections (Steinolfson & Hundhausen 1988; Wang et al. 1995) as compared to the static initial state because the former includes consistently coronal expansion and resembles the observed features of the preevent corona.

With a helmet streamer as the initial state, many attempts have been made to simulate the initiation of CMEs, either by photospheric shearing (Linker & Mikic', 1995), magnetic flux emergence (Guo et al. 1991; Steinolfson 1992), or thermal energy release in a heated corona (Steinolfson & Hundhausen 1988), and considerable progress has been made. However, little attention has been paid to the internal structure of helmet streamers in these numerical simulations, although there is observational evidence that a helmet streamer indeed exhibits complicated magnetic structures, e.g., the cavity situated below the streamer dome and the quiescent prominence inside the cavity (Pneuman & Orrall 1986; Low 1994). The magnetic structure in the closed region of the streamer is very important because it determines both the equilibrium of the streamer and the magnetic free energy in the preevent corona needed to fuel CMEs. Aly (1984, 1991) showed that if a force-free magnetic field were to be anchored to the surface of the Sun, it cannot have an energy in excess of that in the corresponding fully open configuration. Low & Smith (1993) interpreted Aly's constraint to mean that, for anchored fields, the field-aligned currents cannot store enough energy to fuel the CME, and they proposed that magnetic energy in the form of detached magnetic fields with cross-field currents may be the source of the total mass-ejection energy. They constructed analytically a helmet-streamer solution including a magnetic bubble in its closed field region, but without considering the plasma flow. Low (1994) further suggested that the cavity below the helmet dome may indeed include a detached magnetic flux rope associated with the prominence. In numerical simulations, it is now possible to construct self-consistently a helmet streamer containing a detached magnetic structure via current emergence from the streamer base.

Recently, Wu, Guo, & Wang (1995) (hereafter WGW95) investigated the dynamics of a helmet streamer by moving quasi-statically into the closed field region of the streamer field. They showed, with ideal MHD, that if the emerging

magnetic bubble is sufficiently small, the resulting configuration will be a quasi-equilibrium helmet streamer containing a detached magnetic bubble in the closed field region. If the emerging bubble is large, the solution describes a non-equilibrium state, and after a period of slow evolution, the streamer-bubble system becomes unstable and breaks up dynamically. Their results indicate that a helmet streamer containing a detached magnetic structure in its closed field region has sufficient magnetic free energy to easily go unstable. The quasi-static solution obtained may serve as a preevent corona for CME simulations.

In this paper we shall investigate the dynamic response of a helmet streamer to the emergence of a current from below, but this time with its magnetic field in a direction opposite to the overlying streamer field and include the effect of resistivity. We do not attempt to model the emergence of a specific current, but rather, we are interested in the topological change of the magnetic field of the streamer, as a means to construct more realistic helmet-streamer solutions.

2. NUMERICAL MODEL

2.1. *Governing Equations*

We model the coronal plasma by using the single-fluid, resistive MHD equations in spherical coordinates assuming axisymmetry. The equations are identical to the equations used in WGW95, except for the magnetic induction equation and the energy equation which are modified to include the effects of resistivity, viz.,

$$\frac{\partial \boldsymbol{B}}{\partial t} = \nabla \times (\boldsymbol{V} \times \boldsymbol{B}) - \nabla \times \eta \boldsymbol{J}\,, \tag{1}$$

and

$$\frac{\partial T}{\partial t} = -\nabla \cdot (T\boldsymbol{V}) + (2-\gamma)T\nabla \cdot \boldsymbol{V} + \frac{\gamma - 1}{\rho R}\eta J^2\,, \tag{2}$$

where the current $\boldsymbol{J} = (1/\mu_0)\nabla \times \boldsymbol{B}$, η is the magnetic resistivity, and the other symbols have their usual meanings. Like Wu, Bao, & Wang (1986), we choose for η the following form:

$$\eta = \begin{cases} \alpha(|J| - |J_c|)^2\,, & |J| > |J_c| \\ 0 & |J| < |J_c| \end{cases}, \tag{3}$$

where α is a constant which scales with Spitzer's classical resistivity α_0, and J_c is the magnitude of the critical current above which the resistivity becomes effective. Physically, this corresponds to some microscale instability that could enhance the resistivity by several orders of magnitude over the classical value when the current intensity exceeds the critical value (Song, Wu, & Dryer 1989). In our computation, we choose $\alpha = 6.94 \times 10^9 \alpha_0$ and $J_c = 1.14 \times 10^{-6}$ A m^{-2}. Some comments about the magnetic resistivity in our model are presented in § 4.

The computational domain extends from $1R_s$ to $7R_s$, where R_s is the solar radius, and from the pole ($\theta = 0°$) to equator ($\theta = 90°$). We use a nonuniform grid in the r-direction, $\Delta r_i = 0.025 r_{i-1}$ and a uniform grid in the meridional direction, $\Delta\theta = 1°.5$, to obtain a grid of 80×63 elements. The MHD equations are discretized by the combined difference scheme (WGW95), and the method of projected normal characteristics (Wu & Wang 1987) are used to treat the boundary conditions. At the equator and the pole symmetric boundary conditions are used; at the inner and outer boundaries characteristic boundary condition and linear extrapolation are used, respectively.

In order to investigate the dynamic response of the helmet streamer to the emergence of a current, we first construct a quasi-equilibrium helmet streamer by using the relaxation method (Steinolfson et al. 1982). The parameters of the streamer are the same as in WGW95. The plasma parameters at the inner boundary are $n_0 = 3.2 \times 10^8$ cm^{-3}, $T_0 = 1.8 \times 10^6$ K, $B_0 = 2.0$ G (i.e., the initial value of plasma-β is 1.0 at the equator and 0.25 at the pole). The magnetic field lines and velocities of the initial streamer are shown in Figure 1.

In the second step, we construct a current-carrying magnetic bubble and move it quasi-statically into the closed region of the streamer to simulate the current-emergence process. To represent the two-dimensional current-carrying magnetic bubble, we assume an equilibrium axisymmetrical cylinder of radius a containing a volumetric current. Using local cylindrical coordinates (r', θ', z), and solving the equilibrium equations, we obtain the pressure and the magnetic field (see WGW95) in the form

$$p(r') = p_0 + \mu_0 j_0^2(\tfrac{1}{18}a^4 - \tfrac{1}{4}a^2 r'^2 + \tfrac{5}{18}ar'^3 - \tfrac{1}{12}r'^4)\,, \tag{4}$$

and

$$\boldsymbol{B}(r') = -\mu_0 j_0(\tfrac{1}{2}ar' - \tfrac{1}{3}r'^2)\boldsymbol{e}_{\theta'}\,, \tag{5}$$

where

$$j_0^2 = \frac{18(m-1)p_0}{\mu_0 a^4}\,,$$

and p_0 is the plasma pressure at the inner boundary.

To implement the current-emergence process, we transform the expressions for p and B from local cylindrical coordinates to global spherical coordinates (see WGW95). This transformation introduces a small error [$\nabla \cdot B/(B_0/R_s) < 0.005$] to the solenoidal condition of the magnetic field. To assure that the solenoidal condition is satisfied, we have employed the iterative divergence-cleaning procedure (Ramshaw 1983) in our computation.

The process of the current emergence is accomplished as follows. First, we place the current-carrying magnetic bubble below the inner boundary ($r = 1R_s$) with its center at

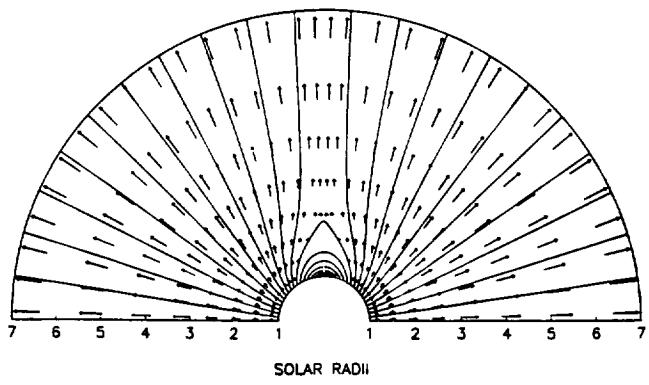

FIG. 1.—Magnetic field lines and velocity field of the initial helmet streamer.

$r = R_s - a$. We then move it very slowly, with respect to the Alfvén velocity, v_A, into the computational domain at constant speed ($v_b \ll v_A$). We choose approximately 4 hr for the bubble to move completely into the closed region of the streamer by adjusting v_b according to the size of the bubble in order to maintain the system in a quasi-equilibrium state. As soon as the current-carrying structure is inside the closed region of the streamer, we let the full set of MHD equations evolve and derive the numerical results. It should be noted that the lower boundary conditions are also computed at each time step in accordance with the method of characteristics (Wu & Wang 1987). The numerical results are given in the next section.

3. NUMERICAL RESULTS

In this study we have computed three cases with different sizes of the bubble radius leading to different levels of the energy (or current intensity) contained in these magnetic bubbles. Subsequently, we obtain three distinct solutions as shown in Figure 2, representing three different states, viz., (1) an eruptive, (2) a nonequilibrium, and (3) a quasi-equilibrium state. The detailed physical results for the three cases are discussed below.

3.1. *Eruptive Case*

In this case we choose $a = 0.15R_s$, for the size of the bubble which possesses a magnetic energy of 1.57×10^{30} ergs, and an initial velocity $v_b = 14.5$ km s^{-1} (i.e., $0.06v_A$). The evolution of the magnetic field and the velocity as well as of the current and density for $t = 4, 5, 6, 7$ hr are shown in Figure 3. We see that the emerging current quickly disrupts the initial helmet streamer. Because the field lines of the emerging field are in a direction opposite to the field lines of the streamer, a current sheet forms between the upper half of the bubble and the streamer field. Figures 3*a*, 3*b*, and 3*c* show an amplified view of the lower part of the computational region. It is clear that two *x*-type neutral points form on the flanks of the bubble where the current density is maximum. Magnetic resistivity causes the field lines to reconnect, and the velocity at the two ends of the reconnected region shows that the reconnected field is moving away from the reconnection region. The top of the erupting current loop reaches a speed of 170 km s^{-1} at $4.5R_s$, while reconnection is still occurring at the flanks of the bubble.

The corresponding relative density contours show that the largest density enhancement occurs at the side of the loop where the current is large, while the top of the loop has a relatively small density enhancement and current.

To illustrate the later phase of the eruption we have plotted field lines and vector velocities at 10 and 20 hr after the current emergence shown in Figure 4. We see that the streamer is disrupted by the passage of the bubble, and that, after the disturbance has propagated out of the domain, the streamer returns to its initial state at $t = 20$ hr.

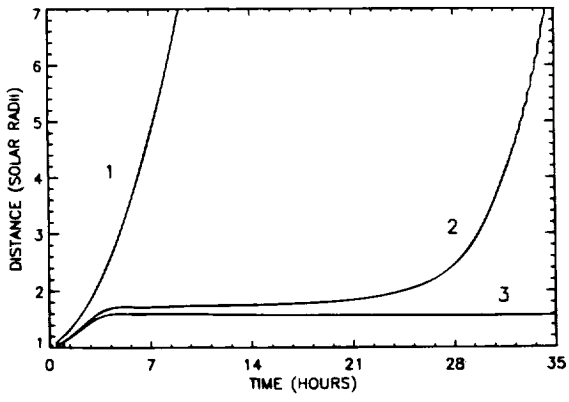

FIG. 2.—Evolution of the position of the neutral point at equator between preexisting field and the current-induced field in three cases.

3.2. *Nonequilibrium Case*

In this case the bubble size is taken to be $0.07R_s$, the magnetic energy is 3.41×10^{29} ergs, and the velocity v_b is 6.77 km s^{-1} (i.e., $0.028v_A$).

Figure 5 shows an amplified view of the topology change of the magnetic field in the closed region of the streamer for this case. We notice that the reconnection process is much slower than in case 1. At $t = 2$ and 4 hr there is no obvious reconnection occurring at the bubble sides. However, as time elapses the effect of the reconnection becomes clear, in that the two *x*-type neutral points at the flanks of the emerging bubble move closer and the emerging current slowly dissipates. Finally, the two *x*-type neutral points merge into one and the emerging current degenerates into a point. At the same time the current existing above the upper half of the emerging bubble expands, forming a new bubble structure above the degenerated current. The field direction of the new bubble is the same as that of the overlying streamer field. The new configuration resembles magnetic field conditions in an inverse-polarity prominence (Leroy, Bommier, & Sahal-Bréchot 1984).

Figure 6 shows the evolution of the magnetic field and velocity from 1 to $7R_s$. Comparing Figures 5 and 6 we realize that as the magnetic topology in the closed region of the streamer evolves, the overall streamer structure is almost unchanged. After the emerged current degenerates, the new configuration will still experience a stage of slow evolution. Then, at about $t = 24$ hr, the whole structure becomes unstable and breaks up, forming a very elongated, narrow transient. Its relative density contours at 28 hr are shown in Figure 7, defining a transient similar to the coronal jets described by Burkepile & St. Cyr (1993). After the transient has propagated out of the computational domain, the streamer structure recovers after roughly 60 hr (Fig. 6*f*).

3.3. *Quasi-equilibrium Case*

In this case we choose a bubble size $0.06R_s$ giving an amount of magnetic energy of 2.51×10^{29} ergs, and the velocity v_b is 5.80 km s^{-1} (i.e., $0.024v_A$). From Figure 8 we see that the first stage of the evolution is similar to case 2, i.e., the emerging current degenerates into an *x*-type neutral point, and above it the original current sheet expands to form a new bubble. However, because of the smaller input energy contained in the original emerging current, after a stage of slow evolution and restructuring, the final configuration remains quasi-statically in the corona. At this stage, magnetic reconnection is still occurring near the neutral point below the bubble due to the finite magnetic resistivity.

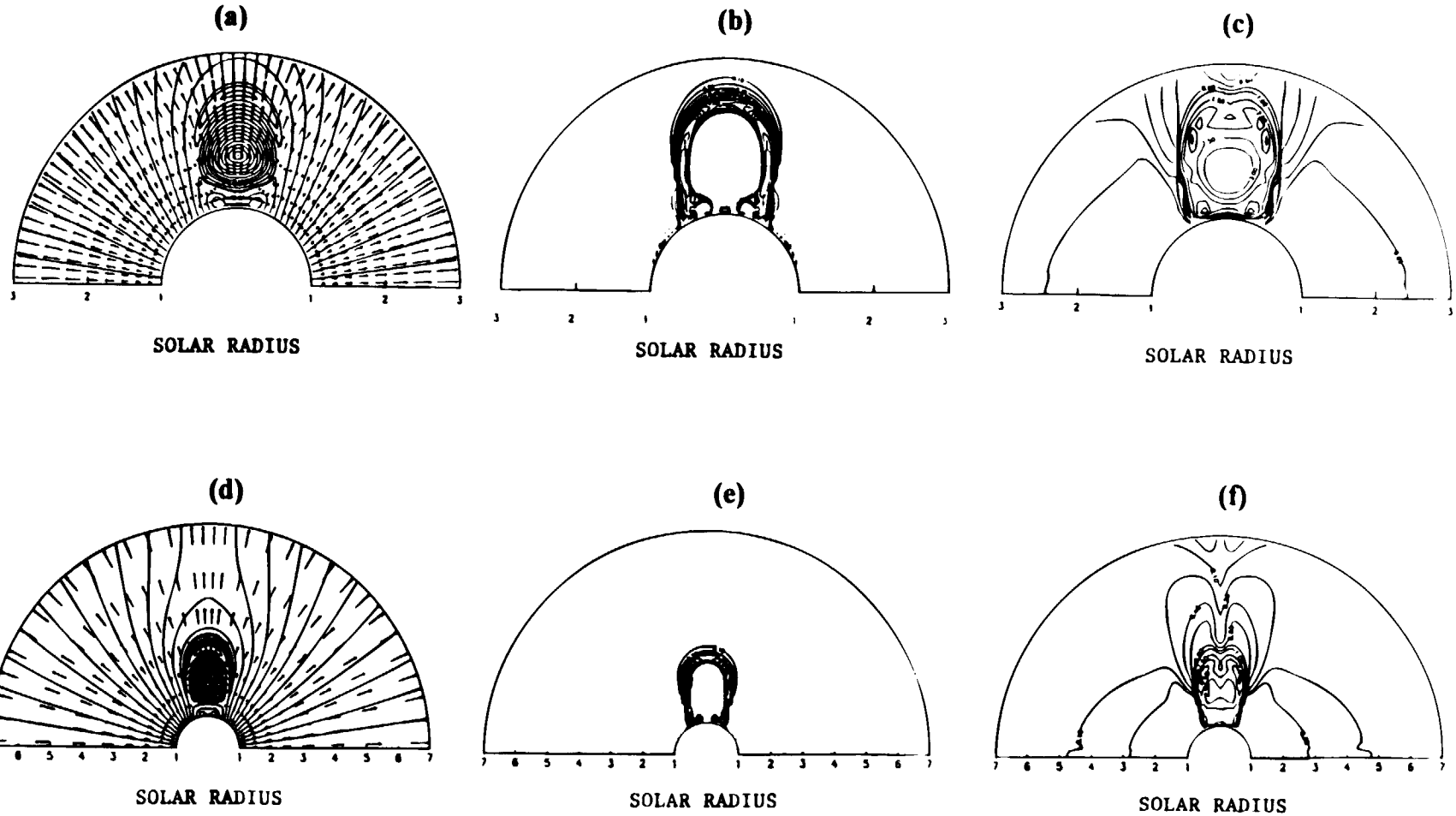

FIG. 3.—Evolution of magnetic field lines, velocity field, current and density in case 1; (*a*) field lines and velocity field at $T = 4$ hr, (*b*) current at $T = 4$ hr, (*c*) density at $T = 4$ hr, (*d*) field lines and velocity field at $T = 5$ hr, (*e*) current at $T = 5$ hr, (*f*) density at 5 hr, (*g*) field lines and velocity field at $T = 6$ hr, (*h*) current at $T = 6$ hr, (*i*) density at $T = 6$ hr, (*j*) field lines and velocity field at $T = 7$ hr, (*k*) current at $T = 7$ hr, and (*l*) density at $T = 7$ hr.

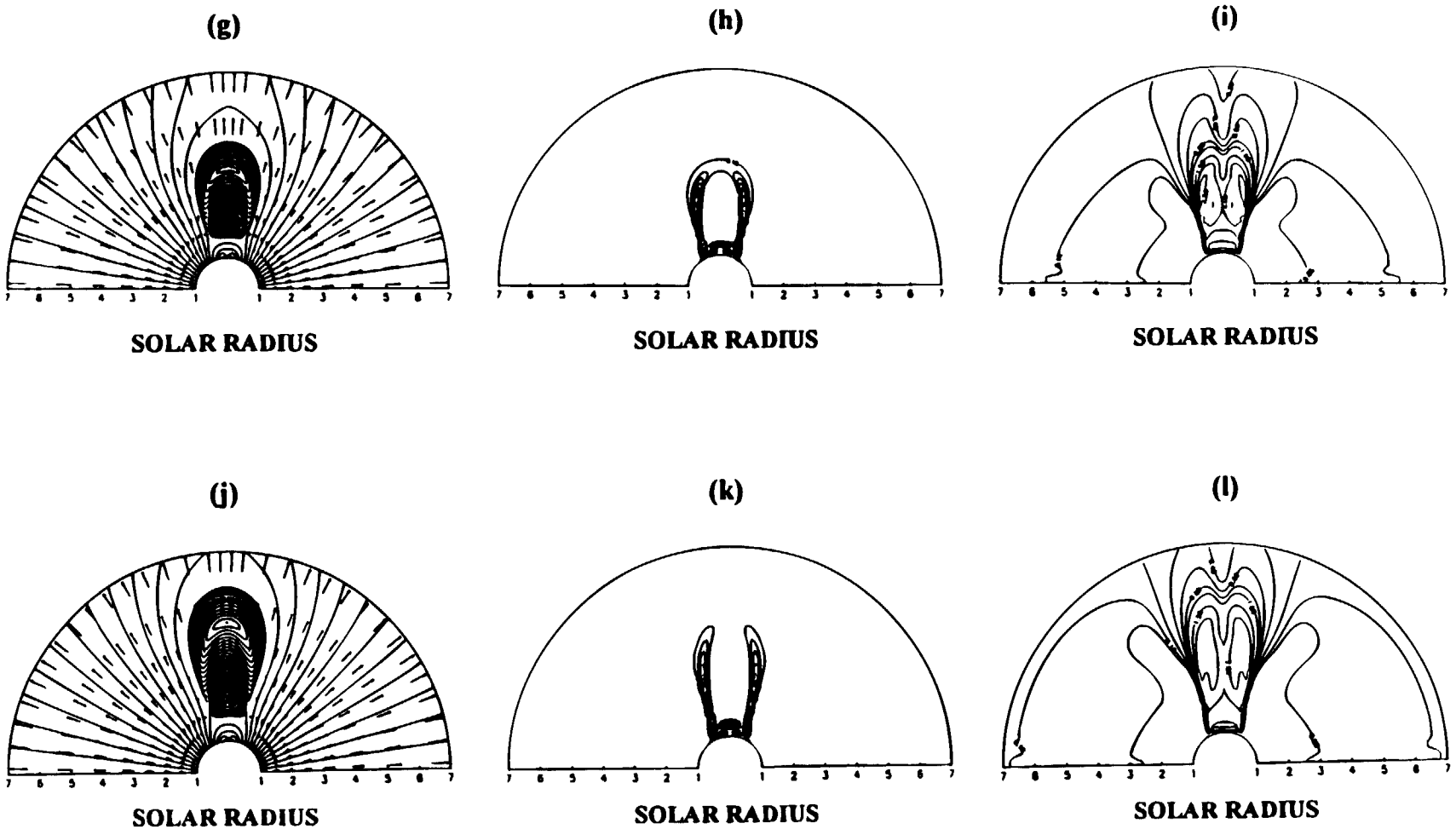

FIG. 3.—*Continued*

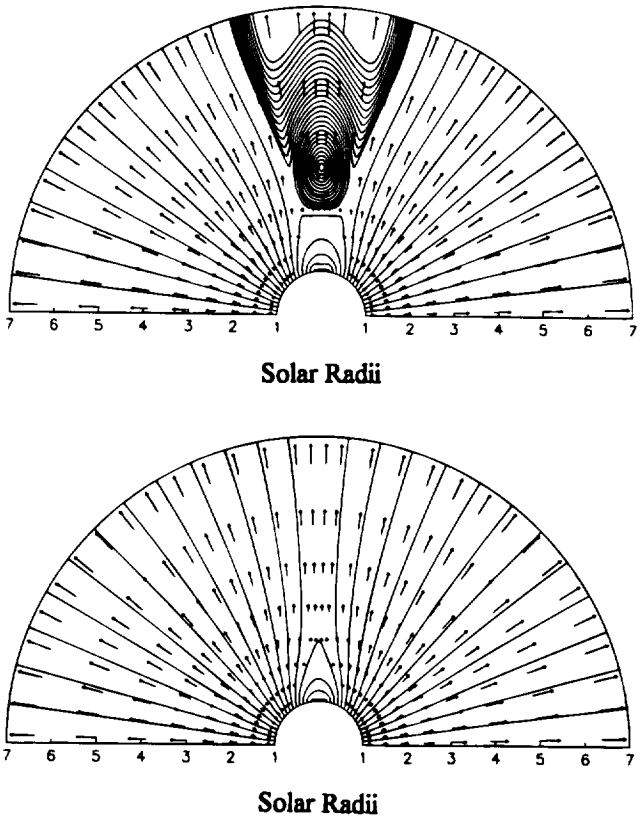

FIG. 4.—Evolution of magnetic field lines and velocity vectors at $T = 10$ hr (*top*) and $T = 20$ hr (*bottom*) for case 1.

Hence the bubble structure slowly dissipates, and the dissipation rate depends on the magnitude of the magnetic diffusivity, η.

4. DISCUSSION

4.1. *Operating Forces*

To discuss the dynamic processes that cause the bubble-destabilization of the streamer, we have plotted in Figure 9 the three relevant forces, i.e., pressure gradient, magnetic force, and gravity, at three locations, as a function of time for case 2. At the lower half of the bubble, Figure 9*a*, the positive pressure-gradient and the magnetic force balance gravity and support the bubble. At the upper half of the bubble, Figure 9*b*, and 9*c*, the pressure-gradient force tends to overcome the combined negative magnetic force and gravity and stretches the closed field lines of the streamer and the force unbalance causes the bubble to move upward. On the other hand, in case 3, the three forces achieve dynamic equilibrium, and the bubble-streamer system is quasi-static. Hence, as pointed out in WGW95, the equilibrium or nonequilibrium state of the bubble is determined by the dynamic interaction of the three forces. However, unlike the simulation in WGW95, where the whole bubble structure emerged from the lower boundary, here the new bubble is formed by the reconnection between the emerging field and the original streamer field. The magnetic confining force, produced by the closed streamer field above the bubble is smaller in the present case because part of the closed streamer field has reconnected and is no longer tied to the solar surface. That is why, in the present case, the bubble-streamer system can lose equilibrium more easily than in the cases studied in WGW95. We find that the equilibrium of the final configuration is very sensitive to the size of the original input current.

One of the noticeable common characteristics in this paper and in WGW95 is that the emerged structure, in a certain parameter range, will first experience a period of slow evolution, then the streamer loaded with this structure loses its equilibrium. This study and WGW95 show that coronal streamers have the ability to be loaded with extra current and mass. The stability of the streamer and loaded structure depends on the dynamic interaction of the three forces as pointed out above. This slow evolutionary stage reflects the restructuring process in the streamer in response to the emerged structure and may explain the slow expansion of streamers prior to their eruption (Illing & Hundhausen 1986).

4.2. *Magnetic Topology*

Using the results of the bubble-streamer interactions, we have studied the changes of magnetic configurations in the closed field region of a streamer. Observations show that quiescent prominences are formed under coronal helmet streamers (Tandberg-Hanssen 1995), and many of these prominences fall in the inverse-polarity category (Leroy et al. 1984). In cases 2 and 3, we have reproduced the basic magnetic configuration of the inverse-polarity prominence in the closed region of a streamer (Figures 5, 6, and 8), and our primary results indicate that such a configuration can easily go unstable. The stability and parameters of this configuration need further investigation, which may elucidate the disparition-brusque phenomenon and its basic relationship to helmet-streamer instabilities.

We have studied the magnetic field development, but a word is necessary concerning the electric current responsible for the bubble configuration. In a fully three-dimensional description the emerging current is connected to the photosphere, under which it forms a closed circuit through, e.g., the convection zone. In our two-dimensional planar configuration we approximate this circuit by considering an emerging current forming a closed loop (an azimuthal current) around the solar equator. This is a reasonable approximation because the axial dimension (the length of a prominence) is much greater than the transverse dimension (the width of a prominence), see, e.g., Tandberg-Hanssen (1995). We also notice that Low & Hundhausen (1995) have pointed out the importance of an azimuthal current in the closed field region of streamers, because such a current running above a prominence is indispensable for the support of the prominence against gravity.

4.3. *Magnetic Resistivity*

The magnetic resistivity in the coronal plasma is very small, while fast reconnection processes are needed to explain the fast magnetic annihilation process occurring in the corona. Numerical simulations have been performed to investigate the details of the reconnection in relatively simple configurations (e.g., Forbes & Priest 1987). However, in our model, the geometry is much more complicated and the magnetic reconnection occurs only in a small portion of the curved sheet. Hence, in our global simulation, we must

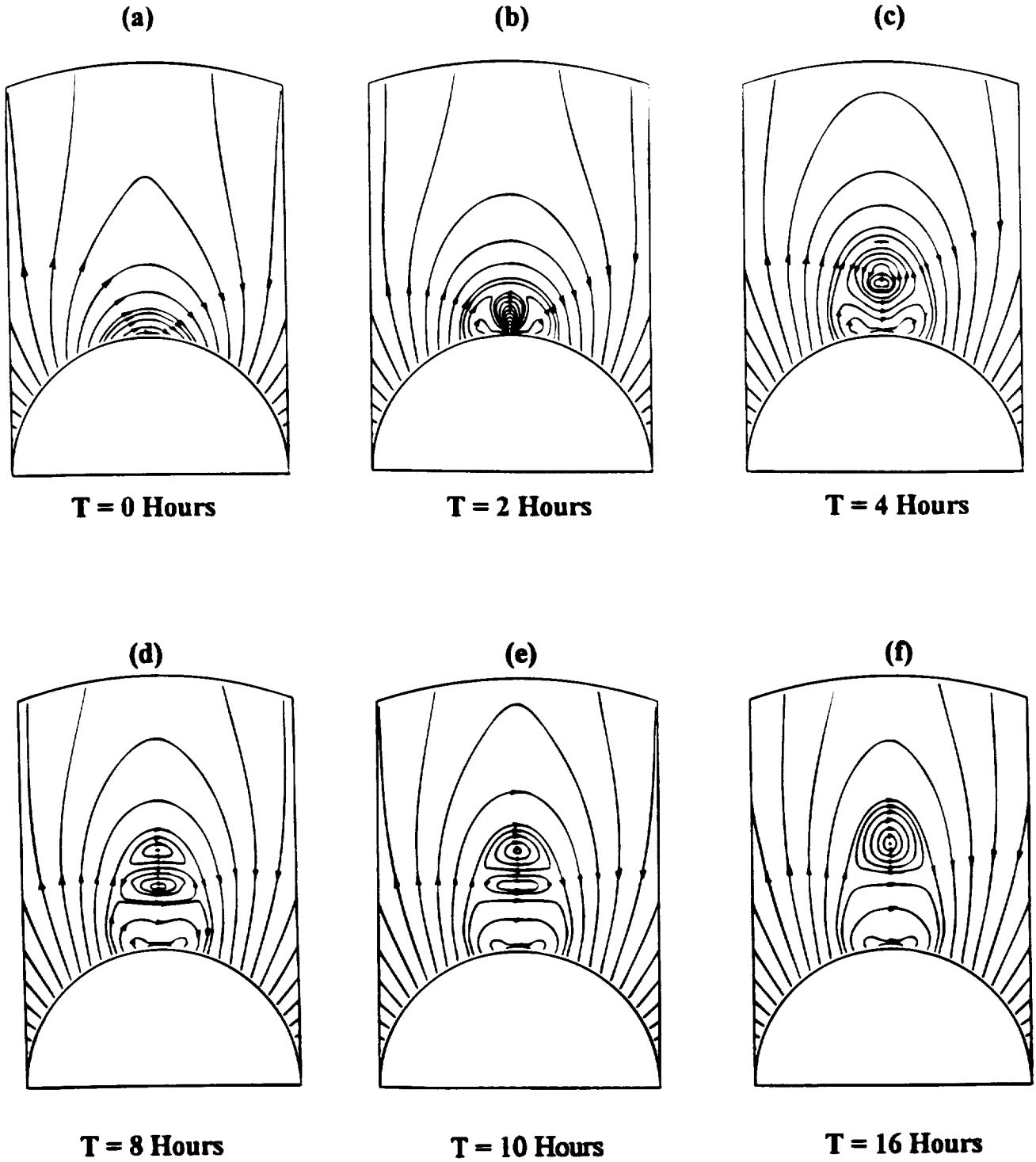

FIG. 5.—Magnetic topology change in the closed field region of the streamer in case 2

assume a reconnection model, (e.g., the one we have chosen in § 2), to simulate the microscale reconnection process occurring in a region that is a few orders of magnitude smaller than the mesh size.

Due to the choice of magnetic resistivity in our model, the magnetic Reynolds number is about 1000 for case 1 and 400 for cases 2 and 3. These Reynolds numbers are much smaller than the magnetic Reynolds number in the real undisturbed corona. The problem of unavoidable increase of resistivity in numerical simulation of magnetic reconnection in solar plasmas is widely recognized and till now, no simulation can accommodate the actual magnetic Reynolds number under coronal conditions. We have performed the simulations using different magnetic resistivity values. We found that different values of η only affect the solution quantitatively, while the basic scenario for the streamer evolution and the field-topology change is the same. The emphasis of this paper is not to investigate the details of the

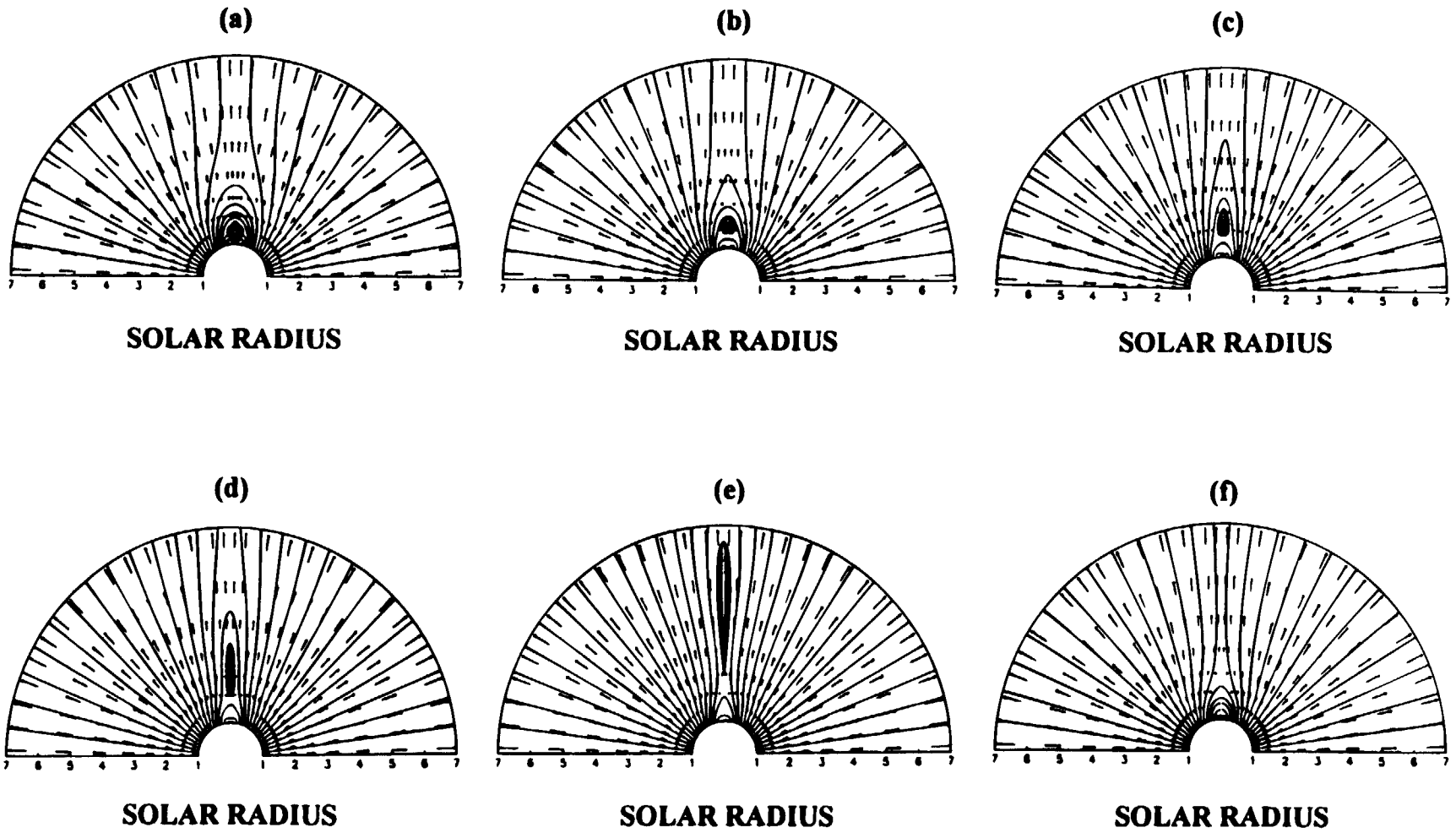

FIG. 6.—Evolution of magnetic field lines and velocity field in case 2; (*a*) $T = 4$ hr, (*b*) $T = 12$ hr, (*c*) $T = 24$ hr, (*d*) $T = 28$ hr, (*e*) $T = 32$ hr, and (*f*) $T = 60$ hr

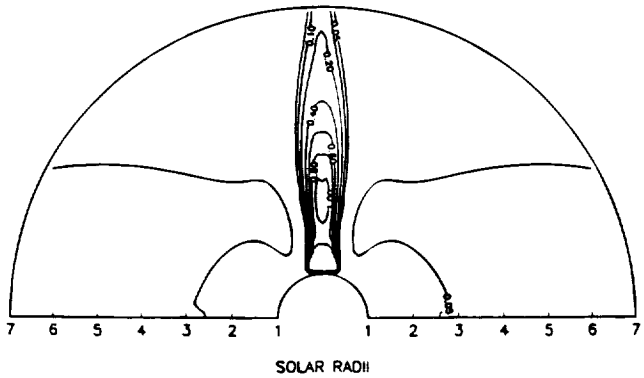

FIG. 7.—Relative density contour at $t = 28$ hr in case 2

reconnection process and energy conversion, but to study the topological change of the streamer field due to current emergence as a means to construct more physically realistic helmet-streamer models. Hence we have chosen to tolerate a small amount of numerical resistivity and some arbitrariness in choosing the reconnection model itself.

5. CONCLUDING REMARKS

We have used a time-dependent, two-dimensional planar MHD model to investigate the dynamic response of a helmet streamer to the emergence of a current with its magnetic field in a direction opposite to the overlying streamer field. Three numerical solutions were found for different values of the current (i.e., size of the magnetic bubble). If the emerging bubble is larger or equal to $0.15R_s$, the solution describes an eruptive case, i.e., the emerging current and the resulting magnetic reconnection occurring at the flanks of the bubble promptly disrupt the original streamer. If the emerging bubble is small, the streamer will experience a stage of slow evolution, in which slow magnetic reconnection leads to a degeneration of the bubble to a neutral point. Above this point, the original current sheet expands to form a new bubble. Depending on the size (i.e., initial input energy) of the bubble, the resulting structure will either remain in situ (for bubble size equals to $0.06R_s$), forming a quasi-static structure, or move upward and disrupt the streamer (bubble size equals to $0.07R_s$), forming a transient similar to observed coronal jets.

Examining Figure 3, we notice that the current contours exhibit a distinct looplike configuration even more so than the density contours. This realization prompts us to suggest that observed coronal loops, in fact, may represent current loops and should not primarily be interpreted as density loops. Density is certainly involved, since physically current is the motion of electrons, and represents the product of electron density and velocity.

Our results demonstrate that current emergence from the base of coronal helmet streamers can be used to construct a

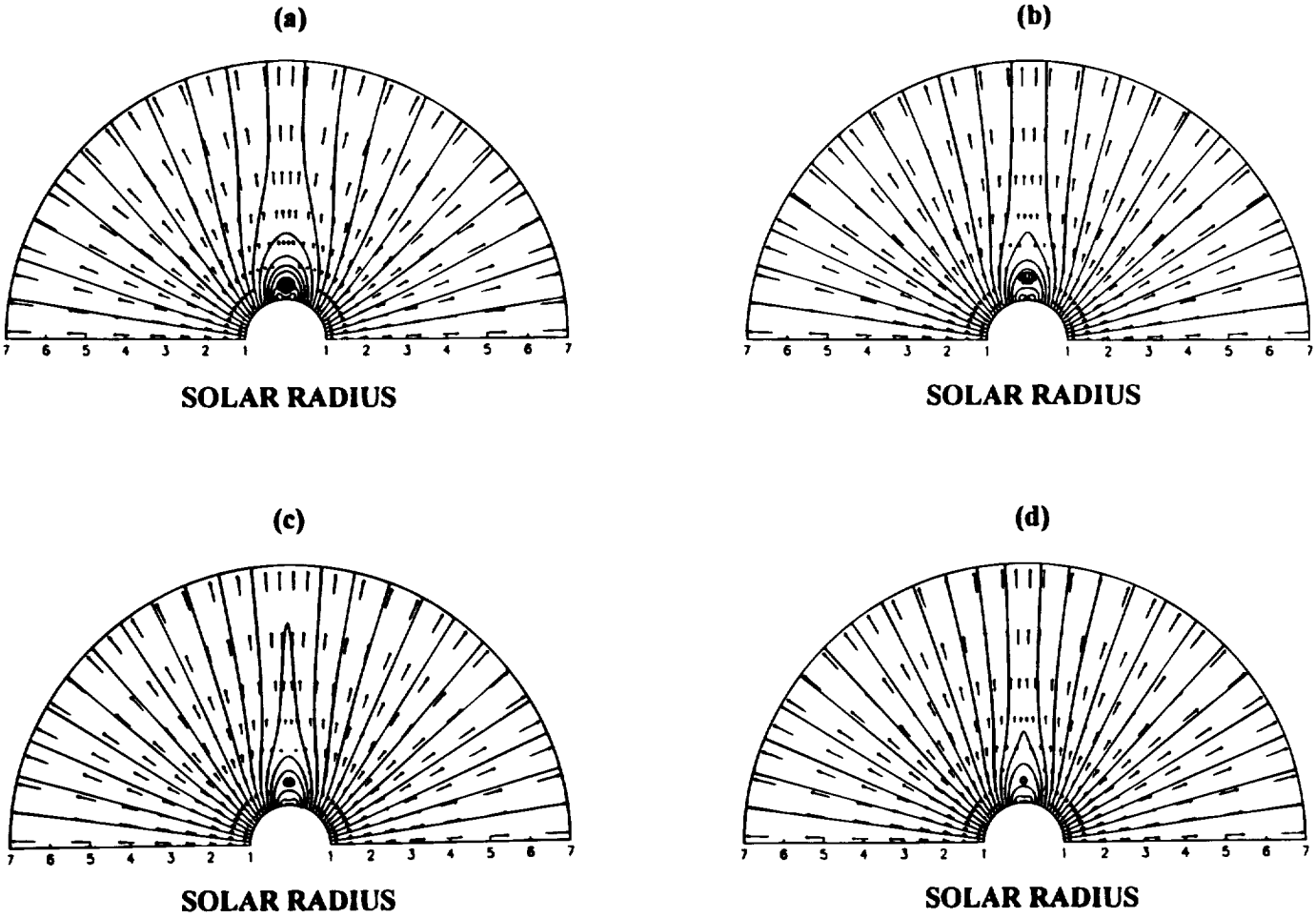

FIG. 8.—Evolution of magnetic field lines and velocity field in case 3; (*a*) $T = 4$ hr, (*b*) $T = 12$ hr, (*c*) $T = 20$ hr, and (*d*) $T = 30$ hr

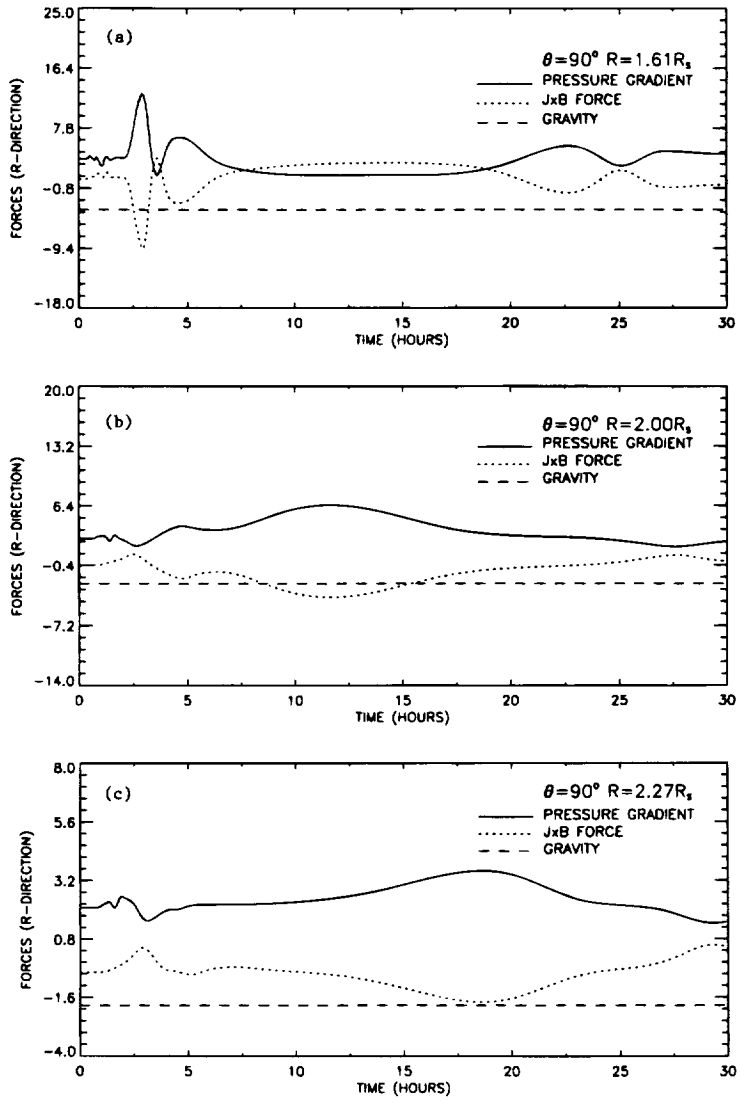

FIG. 9.—Evolution of the relative importance of the three forces for case 2 at three locations; (*a*) below the bubble center, (*b*) above the bubble center, and (*c*) above the bubble in the streamer.

streamer containing detached magnetic structures in its closed field region. This streamer model seems more realistic both from an observational point of view as well as for further discussion of magnetic free energy contained in the preevent streamer. In cases 2 and 3 we reproduce the basic magnetic configuration of an inverse-polarity prominence in the closed region of the streamer. The quasi-equilibrium case (case 3) can be used as preevent corona to study the initiation of CMEs. More parametric studies should be done concerning the stability of the bubble-streamer configuration and the dissipation rate of the quasi-equilibrium bubble in the streamer.

Work done by W. P. G. and S. T. W. was supported by NSF grant ATM 92-15673 and NASA grant NAGW-4665.

REFERENCES

Aly, J. J., 1984, ApJ, 283, 349
———. 1991, ApJ, 375, L61
Burkepile, J. T., & St. Cyr, O. C. 1993, Natl. Cent. Atmos. Research Tech. Note (nr 369 + STR)
Forbes, T. G., & Priest, E. R. 1987, Rev. Geophys., 25, 1583
Guo, W. P., Wang, J. F., Liang, B. X., & Wu, S. T. 1991, in IAU Symp. 133, Eruptive Solar Flares, ed. Z. Švestka, B. V., Jackson, M. E. Machado, (Dordrecht: Reidel), 381
Hundhausen, A. J. 1993, J. Geophys. Res., 98, 13177
Illing, R. M. E., & Hundhausen, A. J. 1986, J. Geophys. Res., 91, 10951
Leroy, J. L., Bommier, V., & Sahal-Bréchot, S. 1984, A&A, 131, 33
Linker, J. A., & Mikic', Z. 1995, ApJ, 248, L45
Low, B. C. 1994, Phys. Plasmas, 1, 1684
Low, B. C., & Hundhausen, J. R. 1995, ApJ, 443, 318
Low, B. C., & Smith, D. F. 1993, ApJ, 410, 412
Pneuman, G. W., & Kopp, R. A. 1971, Sol. Phys., 18, 258
Pneuman, G. W., & Orrall, F. Q. 1986, in Physics of the Sun, Vol. 2, ed. P. A. Sturrock, T. E. Holzer, D. M. Mihalas, & R. K. Ulrich (Dordrecht: Reidel), 100
Ramshaw, J. D. 1983, J. Comp. Phys., 52, 592
Song, M. T., Wu, S. T., & Dryer, M. 1989, Ap&SS, 152, 287
Steinolfson, R. S. 1992, J. Geophys. Res., 97, 10811
Steinolfson, R. S., & Hundhausen, A. J. 1988, J. Geophys. Res., 93, 14269
Steinolfson, R. S., Suess, S. T., & Wu, S. T. 1982, ApJ, 255, 730
Tandberg-Hanssen, E. 1995, The Nature of Solar Prominences, (Dordrecht: Kluwer)
Wang, A. H., Wu, S. T., Suess, S. T., & Poletto, G. 1993, Sol. Phys., 147, 55
———. 1995, Sol. Phys., 161, 365
Wu, S. T., Bao, J. J., & Wang, J. F. 1986, Adv. Space Res., 6, 53
Wu, S. T., Guo, W. P., & Wang, J. F. 1995, Sol. Phys., 157, 325 (WGW95)
Wu, S. T., & Wang, J. F. 1987, Comp. Method Appl. Mech. Eng., 64, 267